2019-05-31

Southern high-latitude warmth during the JurassicCretaceous: New evidence from clumped isotope thermometry

Vickers, ML

10.1130/g46263.1
Geology
Geological Society of America

Southern high latitude warmth during the Jurassic–Cretaceous: New evidence from clumped isotope thermometry

Madeleine L. Vickers[1], David Bajnai[2], Gregory D. Price[3], Jolien Linckens[2], Jens Fiebig[2]

[1] Department of Geosciences and Natural Resource Management, University of Copenhagen, 1350 Copenhagen, Denmark

[2] Institute of Geosciences, Goethe University Frankfurt, 60438 Frankfurt am Main, Germany

[3] School of Geography, Earth & Environmental Sciences, University of Plymouth, PL4 8AA Plymouth, United Kingdom

ABSTRACT

In order to understand the climate dynamics of the Mesozoic greenhouse world, it is vital to determine paleotemperatures from higher latitudes. For the Jurassic and Cretaceous climate, there are significant discrepancies between different proxies and between proxy data and climate models. We determined paleotemperatures from Late Jurassic and Early Cretaceous belemnites using the carbonate clumped isotope paleothermometer and compared these values to temperatures derived from TEX_{86} and other proxies. From our analyses, we infer an average temperature of ca. 25 °C for the upper part of the water column of the Southern Atlantic Ocean. Our data imply that for mid to high latitudes, climate models underestimate marine temperatures by >5 °C and, therefore, the amount of warming that would accompany an increase in atmospheric CO_2 of more than 4x pre-industrial levels, as is projected for the near future.

INTRODUCTION

Modern anthropogenic CO_2 production has resulted in rapid climate change, with near-surface air temperatures in the high latitude regions rising at ca. twice the global average rate (Screen and Simmonds, 2010). Predictions of how global and polar temperatures will change over

the next few decades in response to continued CO_2 release may be improved by studying past climate response to elevated CO_2 levels. The Late Jurassic to Early Cretaceous (164 to 100 million years ago) was characterized by extremely high but variable levels of atmospheric CO_2 (from ca. 2x to 8x pre-industrial levels; Wang et al., 2014; Foster et al., 2017), yet reconstructions of marine temperatures, particularly for the high latitudes, are contradictory (e.g., Huber et al., 1995; Price and Gröcke, 2002; Bice et al., 2003; Poulsen, 2004; Jenkyns et al., 2012; Price and Passey, 2013; O'Brien et al., 2017).

The stable oxygen isotope composition of the carbonate remains of marine organisms is the most extensively used temperature proxy, yet high-latitude sea-surface temperatures (SST) derived from independent organic geochemical paleothermometers, i.e., TEX_{86}, may be ca. 10 °C warmer than $\delta^{18}O$-based temperature reconstructions (e.g., Mutterlose et al., 2010; O'Brien et al., 2012) and up to 6 °C warmer than general circulation model (GCM) predictions (Price and Passey, 2013). These differences have led some authors to suggest that the high TEX_{86} SST estimates are too warm (Hollis et al., 2009; Meyer et al., 2018), and there is an ongoing debate as to which calibration is appropriate for applications of the TEX_{86} proxy at specific regions and different intervals of the geologic record (Kim et al., 2012; Taylor et al., 2013). Conversely, $\delta^{18}O$-based paleotemperature reconstructions rely on several assumptions, among which is the oxygen isotope composition of the seawater ($\delta^{18}O_{sw}$; Huber et al., 1995; Price and Gröcke, 2002; Bice et al., 2003), and the accuracy of these assumptions still needs to be verified. If the interpretation of warm sub-polar paleo-ocean temperatures can be confirmed, they imply that past and future polar warming may be much greater (i.e., >5 °C) than indicated by climate models. Furthermore, such warm temperatures test the veracity of claims of Early to mid-Cretaceous polar ice, in particular from those studies deriving data from locations distal to the poles (Miller, 2009).

Deep Sea Drilling Project Site 511, on the Falkland Plateau (51°00.28'S, 46°58.30'W), is particularly well suited for studying Jurassic and Cretaceous climate due to its abundant, exceptionally preserved macrofossils, including belemnites (Jeletzky, 1983; Price and Sellwood, 1997; Price and Gröcke, 2002). The Falkland Plateau was located at approximately 53 °S during the Late Jurassic–Early Cretaceous (Scotese, 2014; Fig. 1). Mean annual temperatures derived from GCMs for the Late Jurassic and Early Cretaceous indicate that the temperatures of the Falkland Plateau region (avg. 10–22 °C) are representative of similar southern hemisphere paleolatitudes (Lunt et al., 2016). Earlier research at Site 511 used the TEX_{86}^{H} paleotemperature proxy to suggest that warm sea-surface conditions (26–35 °C) existed during the Late Jurassic–Early Cretaceous interval (Jenkyns et al., 2012). These paleotemperatures are consistently warmer than paleotemperature estimates based on $\delta^{18}O_{belemnite}$, assuming a $\delta^{18}O_{sw}$ of -1‰ SMOW (11–21 °C; Price and Gröcke, 2002). Another study, undertaken on Barremian to Aptian sediments from two outcrops in northern Germany, also shows that $\delta^{18}O_{belemnite}$-derived paleotemperatures (12–16 °C) are consistently cooler than TEX_{86}-based estimates (26–32 °C; Mutterlose et al., 2010). Jenkyns et al. (2012) argue that the offset is due to TEX_{86} recording sea surface temperatures, whereas belemnites record temperatures from deeper water, possibly from below the thermocline.

In this study, we apply the carbonate clumped isotope paleothermometer to exceptionally well-preserved belemnite rostra from Site 511. This proxy provides seawater temperature estimates independent of $\delta^{18}O_{sw}$ (Price and Passey, 2013; Wierzbowski et al., 2018). In addition to constraining high latitude temperatures, we set out to resolve the uncertainties associated with previous $\delta^{18}O$-based belemnite temperature reconstructions.

MATERIALS AND METHODS

Stratigraphy and samples

The lithology of the sampled section of Site 511 consists of grey-black, thinly laminated mudstones and soft, grey claystones, which were deposited in a periodically anoxic, low-energy, shallow (< 400 m) basin (Basov and Krasheninnikov, 1983; Jeletzky, 1983).

A geothermal gradient of 7.4 °C/100 m has been determined (Langseth and Ludwig, 1983) at Site 511, thus, for the samples analyzed in this study, we can estimate a maximum burial temperature of ca. 50 °C. At elevated temperatures, diffusion of carbon and oxygen isotopes in the carbonate mineral lattice may reset the initial bond-ordering (e.g., Henkes et al., 2014). However, theoretical calculations based on laboratory experiments provide evidence that solid-state diffusion, even in wet and high-pressure conditions, is insignificant below 100 °C burial temperatures on a timescale of 100–160 Ma (Passey and Henkes, 2012). Thus, it is unlikely that the belemnite rostra analyzed in this study were affected by solid-state reordering.

Eleven belemnites (*Belemnopsis* sp.) were selected for maximum stratigraphic coverage and were geochemically screened to include the best-preserved samples, as indicated by available trace element concentrations (i.e., low Fe and Mn; high Sr and Mg concentrations; Price and Gröcke, 2002; Supplemental Information) and cathodoluminescence analyses (Figure 5 of Price and Sellwood, 1997). Subsamples were derived avoiding the margins and apical zone, as these areas are much more susceptible to diagenetic overgrowth and cementation, respectively than the rest of the belemnite (e.g., Ullmann et al., 2015). In addition, we made electron backscatter diffraction (EBSD) analyses and secondary electron microscopy (SEM-BSE) images of selected rostra at the Goethe University Frankfurt (Supplemental Information).

Clumped Isotope Analyses

Carbonate digestion (90 °C), CO_2 purification (cryotraps and GC) and subsequent measurement procedures (ThermoFisher MAT 253) are identical to the techniques described in Wierzbowski et al. (2018). Raw isotope values were calculated using the IUPAC isotopic

parameters, and are projected to the CO_2 reference frame ($\Delta_{47\,(RFAC)}$; Petersen et al., 2019). To verify the consistency and precision of the clumped isotope measurements, six carbonate standards (ETH1–4, MuStd, Carrara) were analyzed along the samples (Data S1). We used the in-house Wacker et al. (2014) calibration to convert $\Delta_{47\,(RFAC)}$ values to temperatures (Supplemental Information; Petersen et al. 2019). Temperature uncertainties are based on external 1*SE* (including *t*-value) that is always larger than or identical to the best attainable internal precision as represented by the shot noise limit (0.004–0.005‰).

RESULTS

Electron Microscopy

All investigated rostra, excluding the areas adjacent to the apical line and the surface, are made up of optical calcite and the c-axis of the calcite grains point radially outwards (Figs. S1-S4). The distribution of the crystallographic a-axes also follows a pattern. This is analogous to pristinely preserved rostra (Stevens et al., 2017). Our EBSD and SEM-BSE analyses suggest that recrystallization, which would change the original orientation of the biogenic calcite grains, did not occur in the sampled areas.

Clumped Isotope Analyses

The $\Delta_{47\,(RFAC)}$ values range between 0.690(±0.011)‰ and 0.707(±0.015)‰. The 1*SE* uncertainty for the clumped isotope measurements, calculated from 4–6 replicate analyses are between 0.004‰ and 0.015‰ (mean 0.010‰). The $\Delta_{47\,(RFAC)}$ values yield seawater temperatures ranging between 21 °C and 28 °C (mean 25 °C) and show no significant stratigraphic trend (Fig. 2). The average uncertainty for the reconstructed temperatures is ±4 °C. Steeper-sloped calibrations yield indistinguishable temperatures within ±1*SE* (Data S1).

DISCUSSION

The Δ_{47}-derived temperature range (21–28 °C, mean 25 °C) for the entire section is higher than those temperatures reconstructed via stable oxygen isotope paleothermometry (11–19 °C, mean 16 °C, assuming $\delta^{18}O_{sw}$ = -1‰ SMOW; Price and Gröcke, 2002), and cooler, and rarely within error, of SST estimates derived from TEX_{86} (25–31 °C; Fig. 2; Jenkyns et al., 2012). In this study, as in Jenkyns et al. (2012), we calculate TEX_{86} temperatures using the TEX_{86}^{H} calibration (Kim et al., 2010). Given the shallow-water and high latitude setting of Site 511 TEX_{86}^{H} may yield maximum SST estimates (Schouten et al., 2013; Taylor et al., 2013). In contrast to TEX_{86}^{H}, the linear calibration used of O'Brien et al. (2017) yield ca. 2–3 °C warmer temperatures, whereas the calibrations that assume a non-surface export depth of GDGTs (Kim et al., 2012; Schouten et al., 2013) yield ca. 5–6 °C cooler estimates (Fig. 2). Although the TEX_{86}^{H} proxy is likely the most appropriate for a high latitude setting such as Site 511, there is ongoing discussion and revision of the various calibrations, and ongoing debate as to which calibration should be applied (e.g., Ho et al., 2014; Inglis et al., 2015). The difference between the TEX_{86}^{H} and the Δ_{47}-derived temperatures for Site 511 may be partially resolved by considering a seasonal bias in either proxy. It has been postulated that belemnites, as nektonic cephalopods, reflect mean annual temperatures (MAT; Price and Sellwood, 1997; Mutterlose et al., 2010), while TEX_{86} may indicate summer temperatures, rather than MAT (Leider et al., 2010; Hollis et al., 2012). Nevertheless, our Δ_{47} temperatures suggest that belemnites were calcifying their rostra in the upper part of the water column (<200 m depth), and are broadly consistent with TEX_{86}-derived SSTs, given the uncertainties listed above. Such an interpretation is in alignment with an assumed predator lifestyle in the photic zone for belemnites (Klug et al., 2016).

All three records from Site 511 show less than 7 °C variability across the entire Late Jurassic and Early Cretaceous interval, although the low sampling resolution means it is not possible to derive more detailed information on Jurassic and Cretaceous climate evolution. These

141 data confirm warm Late Jurassic–Early Cretaceous high latitude ocean temperatures, possibly
142 precluding the likelihood of substantial land ice, and are consistent with estimated MATs from
143 fossil plant assemblages from the Antarctic Peninsula (Francis and Poole, 2002). The most likely
144 mechanism to account for such warmth observed at Site 511 is high atmospheric greenhouse gas
145 concentrations and high polar heat transport. The shallow meridional temperature gradients of the
146 past greenhouse climates pose a significant challenge to numerical climate models (Huber and
147 Caballero, 2011), in that increased greenhouse gases may yield warm Polar Regions, but also
148 overheat the Tropics. MATs for the Cretaceous derived from coupled ocean-atmosphere climate
149 models provide estimates for 53 °S ranging from 12 °C to 21 °C (Zhou et al., 2008; Donnadieu et
150 al., 2016). The higher of these estimates are generated with 2240 ppm pCO_2 (8 x pre-industrial
151 levels; Donnadieu et al., 2016). These atmospheric CO_2 concentrations typically exceed estimates
152 of Cretaceous pCO_2 derived from fossil leaf stomatal index measurements, isotope-based or
153 geochemical model estimates (Wang et al., 2014; Foster et al., 2017).
154 Furthermore, it is crucial to consider the magnitude of a non-CO_2 component of local
155 climate change, before proxies from a single site are interpreted in a global context (Lunt et al.,
156 2016). GCM output indicates warm conditions during the Cretaceous at Site 511 when compared to
157 the Eocene (Lunt et al., 2016), with almost invariable modeled global mean temperatures over the
158 same period, when pCO_2 is kept constant. This suggests that contributions from other processes
159 (e.g., paleogeography) may account for some of the observed warmth. Despite these findings and
160 those of others (Donnadieu et al., 2016), the role of paleogeography in regulating climate remains
161 less than clear.
162 Such warm temperatures at Site 511 challenge our understanding of how the ocean-
163 atmosphere system operated in the past (Poulsen, 2004) and may also have important implications
164 for the prediction of future climates as they imply we may be underestimating future climate change

in such regions (Spicer et al., 2008). Proposed mechanisms to increase the transfer of heat toward the poles (Schmidt and Mysak, 1996), including sensible and latent heat transfer via the atmosphere and heat transfer via the oceans (Hotinski and Toggweiler, 2003), are hence implied. As Site 511 was situated in a seaway open to the southwest (Fig. 1), increased heat transfer via warm ocean currents can only be derived from the Pacific. Thus, other processes, including heat transfer via the atmosphere, might also be important for this region.

These new warm Δ_{47}-derived temperature reconstructions also have implications for basin-scale hydrologies. In conjunction with the $\delta^{18}O_{belemnite}$ data (Price and Sellwood, 1997; Price and Gröcke, 2002), we can estimate $\delta^{18}O_{sw}$, assuming the temperature dependence of oxygen isotope fractionation between belemnite calcite and seawater corresponds to Kim and O'Neil (1997). The $\delta^{18}O$–temperature equation of Kim and O'Neil (1997) indicates that $\delta^{18}O_{sw}$ may have averaged +1.0‰ SMOW (1*SE* = 0.7‰; Fig. 2, Data S1), heavier than the global average for an ice-free world (-1‰ SMOW; Shackleton and Kennett, 1975). This could suggest that the semi-enclosed basin in which Site 511 was located was dominated by evaporation; alternatively, it is quite possible that the Kim and O'Neil (1997) calcite equation is not applicable to belemnite calcite.

CONCLUSIONS

This proxy-to-proxy intercomparison reduces the uncertainty on temperature estimates for the Mesozoic high southern latitudes. Our Δ_{47}-derived temperatures, although slightly cooler, are consistent with the TEX_{86}^{H} reconstructions for sea-surface temperatures. The new Δ_{47} data, in conjunction with $\delta^{18}O_{belemnite}$ data imply local $\delta^{18}O_{sw}$ values of ca. 1.0(±0.7) ‰ SMOW, indicating a strong role of evaporation on the Falkland Plateau, which was a semi-enclosed basin during the Late Jurassic and Early Cretaceous. The warm reconstructed paleotemperatures, if extrapolated poleward, reinforce evidence of temperate polar conditions and lack of polar ice. If these warm ocean temperatures, occurring when pCO_2 in Earth's atmosphere were also high, prove accurate,

they may indicate that greenhouse gases could have heated the oceans during the Jurassic and Cretaceous more than currently accepted. This suggests that future warming from elevated atmospheric CO_2 concentrations may be much greater than that predicted by models.

ACKNOWLEDGMENTS

We thank C. John (Imperial College, London), S. Hofmann, C. Schreiber (Goethe University Frankfurt), N. Löffler, K. Methner, E. Krsnik (Senckenberg BIK-F), D. Gröcke (Durham University), S. Robinson (University of Oxford) and our anonymous reviewers. Funding was provided by a PhD scholarship from the University of Plymouth, UK, and a European Consortium for Ocean Research Drilling (ECORD) grant to M.V.; a UK Natural Environment Research Council (NERC) grant (NE/J020842/1) to G.D.P.; and the European Union's Horizon 2020 research and innovation program under the Marie Skłodowska-Curie grant agreement No. 643084 (BASE-LiNE Earth) to B.D and J.F.

REFERENCES CITED

Basov, I. A., and Krasheninnikov, V., 1983, Benthic foraminifers in Mesozoic and Cenozoic sediments of the southwestern Atlantic as an indicator of paleoenvironment, Deep Sea Drilling Project Leg 71: Initial Reports of the Deep Sea Drilling Project, v. 71, p. 739-787.

Bice, K. L., Huber, B. T., and Norris, R. D., 2003, Extreme polar warmth during the Cretaceous greenhouse? Paradox of the late Turonian $\delta^{18}O$ record at Deep Sea Drilling Project Site 511: Paleoceanography, v. 18, no. 2.

Donnadieu, Y., Pucéat, E., Moiroud, M., Guillocheau, F., and Deconinck, J.-F., 2016, A better-ventilated ocean triggered by Late Cretaceous changes in continental configuration: Nature communications, v. 7, p. 10316.

Foster, G. L., Royer, D. L., and Lunt, D. J., 2017, Future climate forcing potentially without precedent in the last 420 million years: Nature Communications, v. 8, p. 14845.

213 Francis, J. E., and Poole, I., 2002, Cretaceous and early Tertiary climates of Antarctica: evidence
214 from fossil wood: Palaeogeography, Palaeoclimatology, Palaeoecology, v. 182, no. 1, p. 47-
215 64.
216 Henkes, G. A., Passey, B. H., Grossman, E. L., Shenton, B. J., Pérez-Huerta, A., and Yancey, T. E.,
217 2014, Temperature limits for preservation of primary calcite clumped isotope
218 paleotemperatures: Geochimica et cosmochimica acta, v. 139, p. 362-382.
219 Ho, S. L., Mollenhauer, G., Fietz, S., Martínez-Garcia, A., Lamy, F., Rueda, G., Schipper, K.,
220 Méheust, M., Rosell-Melé, A., and Stein, R., 2014, Appraisal of TEX_{86} and TEX_{86}^{L}
221 thermometries in subpolar and polar regions: Geochimica et Cosmochimica Acta, v. 131, p.
222 213-226.
223 Hollis, C. J., Handley, L., Crouch, E. M., Morgans, H. E., Baker, J. A., Creech, J., Collins, K. S.,
224 Gibbs, S. J., Huber, M., and Schouten, S., 2009, Tropical sea temperatures in the high-
225 latitude South Pacific during the Eocene: Geology, v. 37, no. 2, p. 99-102.
226 Hollis, C. J., Taylor, K. W., Handley, L., Pancost, R. D., Huber, M., Creech, J. B., Hines, B. R.,
227 Crouch, E. M., Morgans, H. E., and Crampton, J. S., 2012, Early Paleogene temperature
228 history of the Southwest Pacific Ocean: Reconciling proxies and models: Earth and
229 Planetary Science Letters, v. 349, p. 53-66.
230 Hotinski, R., and Toggweiler, J., 2003, Impact of a Tethyan circumglobal passage on ocean heat
231 transport and “equable” climates: Paleoceanography, v. 18, no. 1.
232 Huber, B. T., Hodell, D. A., and Hamilton, C. A., 1995, Mid to Late Cretaceous climate of the
233 southern high latitudes: stable isotopic evidence for minimal equator-to-pole thermal
234 gradients: Bulletin of the Geological Society of America, v. 107, p. 1164–1191.
235 Huber, M., and Caballero, R., 2003, Eocene El Nino: Evidence for robust tropical dynamics in the"
236 hothouse": Science, v. 299, no. 5608, p. 877-881.

Inglis, G. N., Farnsworth, A., Lunt, D., Foster, G. L., Hollis, C. J., Pagani, M., Jardine, P. E., Pearson, P. N., Markwick, P., and Galsworthy, A. M., 2015, Descent toward the Icehouse: Eocene sea surface cooling inferred from GDGT distributions: Paleoceanography and Paleoclimatology, v. 30, no. 7, p. 1000-1020.

Jeletzky, J., 1983, Macroinvertebrate paleontology, biochronology, and paleoenvironments of Lower Cretaceous and Upper Jurassic rocks, Deep Sea Drilling Hole 511, eastern Falkland Plateau: Initial Reports of the Deep Sea Drilling Project, v. 71, p. 951-975.

Jenkyns, H., Schouten-Huibers, L., Schouten, S., and Sinninghe Damsté, J., 2012, Warm Middle Jurassic-Early Cretaceous high-latitude sea-surface temperatures from the Southern Ocean: Climate of the Past, v. 8, no. 1.

Kim, J.-H., Romero, O. E., Lohmann, G., Donner, B., Laepple, T., Haam, E., and Damste, J. S. S., 2012, Pronounced subsurface cooling of North Atlantic waters off Northwest Africa during Dansgaard–Oeschger interstadials: Earth and Planetary Science Letters, v. 339, p. 95-102.

Kim, J.-H., Van der Meer, J., Schouten, S., Helmke, P., Willmott, V., Sangiorgi, F., Koç, N., Hopmans, E. C., and Damsté, J. S. S., 2010, New indices and calibrations derived from the distribution of crenarchaeal isoprenoid tetraether lipids: Implications for past sea surface temperature reconstructions: Geochimica et Cosmochimica Acta, v. 74, no. 16, p. 4639-4654.

Kim, S.-T., and O'Neil, J. R., 1997, Equilibrium and nonequilibrium oxygen isotope effects in synthetic carbonates: Geochimica et Cosmochimica Acta, v. 61, no. 16, p. 3461-3475.

Klug, C., Schweigert, G., Fuchs, D., Kruta, I., and Tischlinger, H., 2016, Adaptations to squid-style high-speed swimming in Jurassic belemnitids: Biology letters, v. 12, no. 1, p. 20150877.

Langseth, M., and Ludwig, W., 1983, A heat-flow measurement on the Falkland Plateau: Initial Reports of the Deep Sea Drilling Project, v. 71, no. SEP, p. 299-303.

Leider, A., Hinrichs, K.-U., Mollenhauer, G., and Versteegh, G. J., 2010, Core-top calibration of the lipid-based $U^{K'}_{37}$ and TEX_{86} temperature proxies on the southern Italian shelf (SW Adriatic Sea, Gulf of Taranto): Earth and Planetary Science Letters, v. 300, no. 1-2, p. 112-124.

Lunt, D. J., Foster, G. L., O'Brien, C. L., Pancost, R. D., and Robinson, S. A., 2016, Palaeogeographic controls on climate and proxy interpretation: Climate of the Past, v. 12, no. 5, p. 1181.

Meyer, K. W., Petersen, S. V., Lohmann, K. C., and Winkelstern, I. Z., 2018, Climate of the Late Cretaceous North American Gulf and Atlantic Coasts: Cretaceous Research, v. 89, p. 160-173.

Miller, K. G., 2009, Broken greenhouse windows Nature Geoscience, v. 2, p. 465-466.

Mutterlose, J., Malkoc, M., Schouten, S., Sinninghe Damsté, J. S., and Forster, A., 2010, TEX_{86} and stable $\delta^{18}O$ paleothermometry of early Cretaceous sediments: Implications for belemnite ecology and paleotemperature proxy application: Earth and Planetary Science Letters, v. 298, no. 3, p. 286-298.

O'Brien, C. L., Robinson, S. A., Pancost, R. D., Damsté, J. S. S., Schouten, S., Lunt, D. J., Alsenz, H., Bornemann, A., Bottini, C., and Brassell, S. C., 2017, Cretaceous sea-surface temperature evolution: Constraints from TEX_{86} and planktonic foraminiferal oxygen isotopes: Earth-Science Reviews, v. 172, p. 224-247.

Passey, B. H., and Henkes, G. A., 2012, Carbonate clumped isotope bond reordering and geospeedometry: Earth and Planetary Science Letters, v. 351, p. 223-236.

Petersen, S. V., Defliese, W. F., Saenger, C., Daëron, M., Huntington, K. W., John, C. M., Kelson, J. R., Coleman, A. S., Kluge, T., Olack, G. A., Schauer, A. J., Bajnai, D., Bonifacie, M., Breitenbach, S. F., Fiebig, J., Fernandez, A. B., Henkes, G. A., Hodell, D., Katz, A., Kele, S., Lohmann, K. C., Passey, B. H., Peral, M. Y., Petrizzo, D. A., Rosenheim, B. E., Tripati, A.,

285 Venturelli, R., Young, E. D., and Winkelstern, I. Z. 2019, Effects of improved ^{17}O correction
286 on inter-laboratory agreement in clumped isotope calibrations, estimates of mineral-specific
287 offsets, and acid fractionation factor temperature dependence: Geochemistry, Geophysics,
288 Geosystems.
289 Poulsen, C. J., 2004, Palaeoclimate: a balmy Arctic: Nature, v. 432, no. 7019, p. 814-815.
290 Price, G.D., and Sellwood, B., 1997, "Warm" palaeotemperatures from high Late Jurassic
291 palaeolatitudes (Falkland Plateau): Ecological, environmental or diagenetic controls?:
292 Palaeogeography, Palaeoclimatology, Palaeoecology, v. 129, no. 3, p. 315-327.
293 Price, G. D., and Gröcke, D. R., 2002, Strontium-isotope stratigraphy and oxygen-and carbon-
294 isotope variation during the Middle Jurassic–Early Cretaceous of the Falkland Plateau,
295 South Atlantic: Palaeogeography, Palaeoclimatology, Palaeoecology, v. 183, no. 3, p. 209-
296 222.
297 Price, G. D., and Passey, B. H., 2013, Dynamic polar climates in a greenhouse world: Evidence
298 from clumped isotope thermometry of Early Cretaceous belemnites: Geology, v. 41, p. 923-
299 926.
300 Schmidt, G. A., and Mysak, L. A., 1996, Can increased poleward oceanic heat flux explain the
301 warm Cretaceous climate?: Paleoceanography, v. 11, no. 5, p. 579-593.
302 Schouten, S., Hopmans, E. C., and Damsté, J. S. S., 2013, The organic geochemistry of glycerol
303 dialkyl glycerol tetraether lipids: a review: Organic geochemistry, v. 54, p. 19-61.
304 Scotese, C. R., 2014, Atlas of Early Cretaceous Paleogeographic Maps, PALEOMAP Atlas for
305 ArcGIS, volume 2, The Cretaceous, Maps 23-31, Mollweide Projection, PALEOMAP
306 Project, Evanston, IL.
307 Screen, J. A., and Simmonds, I., 2010, The central role of diminishing sea ice in recent Arctic
308 temperature amplification: Nature, v. 464, no. 7293, p. 1334-1337.

309 Shackleton, N., and Kennett, J., 1975, Paleotemperature history of the Cenozoic and the initiation of
310 Antarctic glaciation: oxygen and carbon isotope analyses in DSDP Sites 277, 279, and 281,
311 Washington DC, US Government Printing Office, Initial reports of the deep sea drilling
312 project, 743-755 p.:
313 Spicer, R. A., Ahlberg, A., Herman, A. B., Hofmann, C.-C., Raikevich, M., Valdes, P. J., and
314 Markwick, P. J., 2008, The Late Cretaceous continental interior of Siberia: A challenge for
315 climate models: Earth and Planetary Science Letters, v. 267, no. 1, p. 228-235.
316 Stevens, K., Griesshaber, E., Schmahl, W., Casella, L. A., Iba, Y., and Mutterlose, J., 2017,
317 Belemnite biomineralization, development, and geochemistry: The complex rostrum of
318 Neohibolites minimus: Palaeogeography, palaeoclimatology, palaeoecology, v. 468, p. 388-
319 402.
320 Taylor, K. W., Huber, M., Hollis, C. J., Hernandez-Sanchez, M. T., and Pancost, R. D., 2013, Re-
321 evaluating modern and Palaeogene GDGT distributions: Implications for SST
322 reconstructions: Global and Planetary Change, v. 108, p. 158-174.
323 Ullmann, C., Frei, R., Korte, C., and Hesselbo, S. P., 2015, Chemical and isotopic architecture of
324 the belemnite rostrum: Geochimica et Cosmochimica Acta, v. 159, p. 231-243.
325 Wacker, U., Fiebig, J., Tödter, J., Schöne, B. R., Bahr, A., Friedrich, O., Tütken, T., Gischler, E.,
326 and Joachimski, M. M., 2014, Empirical calibration of the clumped isotope
327 paleothermometer using calcites of various origins: Geochimica et Cosmochimica Acta, v.
328 141, p. 127-144.
329 Wang, Y., Huang, C., Sun, B., Quan, C., Wu, J., and Lin, Z., 2014, Paleo-CO_2 variation trends and
330 the Cretaceous greenhouse climate: Earth-Science Reviews, v. 129, p. 136-147.

Wierzbowski, H., Bajnai, D., Wacker, U., Rogov, M. A., Fiebig, J., and Tesakova, E. M., 2018, Clumped isotope record of salinity variations in the Subboreal Province at the Middle–Late Jurassic transition: Global and Planetary Change.

Zhou, J., Poulsen, C., Pollard, D., and White, T., 2008, Simulation of modern and middle Cretaceous marine $\delta^{18}O$ with an ocean-atmosphere general circulation model: Paleoceanography, v. 23, no. 3, p. PA3223.

338

339 **FIGURE CAPTIONS**

340 **Figure 1.** Paleogeographic setting of the Deep Sea Drilling Project Site 511. Early Cretaceous

341 paleogeographic reconstruction after Scotese (2014).

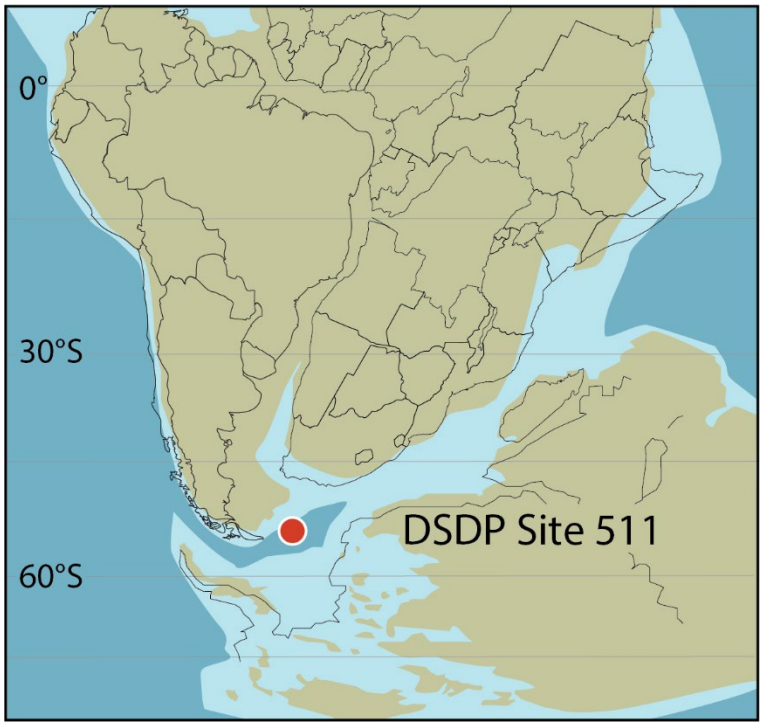

Figure 2. Jurassic and Early Cretaceous temperatures and seawater $\delta^{18}O$ from DSDP Site 511. **(A)** Clumped isotope seawater temperature reconstructions for Site 511 (this study) are compared to those based on $\delta^{18}O_{belemnite}$ (Price and Gröcke, 2002; Price and Sellwood, 1997; plotted using Kim and O'Neil, 1997, with an assumed $\delta^{18}O_{sw}$ of -1‰ SMOW) and TEX_{86} (Jenkyns et al., 2012). Infilled green circles represent $\delta^{18}O_{belemnite}$ temperatures from Price and Gröcke (2002), hollow green circles are the belemnites that were also used for clumped isotopes analysis in this study. For TEX_{86} temperatures, dotted lines used $TEX_{86}^{H,0\text{-}200}$ (Kim et al. 2012., eq. 2), dashed used $TEX_{86\text{-}linear}$ (O'Brien et al., 2017, eq. 4), and solid line and points used the TEX_{86}^{H} calibration (Kim et al. 2010, eq.10). **(B)** Reconstructed $\delta^{18}O_{sw}$ values (this study) using the equation of Kim and O'Neil (1997). Error bars represent for $\delta^{18}O_{belemnite}$ and Δ_{47} the 1*SE* of multiple replicate analyses; for TEX_{86}^{H} the calibration error; and for $\delta^{18}O_{sw}$ the 1*SE*. corresponding to the Δ_{47} measurements. Age model construction is described in the Supplemental Information, whereas data for this figure can be found in Data S1.